Algal Research 27 (2017) 55–64

Contents lists available at ScienceDirect

Algal Research

journal homepage: www.elsevier.com/locate/algal

Outdoor performance of *Chlorococcum littorale* at different locations

Iago Teles Dominguez Cabanelas[a,*], Petronella M. Slegers[d], Hanna Böpple[b], Dorinde M.M. Kleinegris[b], René H. Wijffels[a,c], Maria J. Barbosa[a]

[a] Wageningen University, Bioprocess Engineering, AlgaePARC, P.O. Box 16, 6700 AA Wageningen, Netherlands[1]
[b] Uni Research Environment, P.B. 7810, 5020 Bergen, Norway
[c] Faculty Biosciences and Aquaculture, Nord University, N-8049 Bodø, Norway
[d] Wageningen University, Biobased Chemistry and Technology, P.O. Box 17, 6700 AA, Wageningen, Netherlands

ARTICLE INFO

Keywords:
Microalgae
Tag
Chlorococcum Littorale
Strain improvement
Modelling carbon partitioning
Outdoor productivities
Year round productivities

ABSTRACT

Our goal in the present study was to evaluate the potential for lipid production of two cell populations of the marine microalgae *Chlorococcum littorale* under different climate conditions. We selected, in a previous study and via fluorescence activated cell sorting (FACS), a new cell population of *Chlorococcum littorale*, namely S5. S5 showed a stable doubled triacylglycerol (TAG) productivity in comparison with the original population. A previously developed model was expanded to include day:night cycles and validated to predict biomass and outdoor TAG productivities at different locations. Four different locations were chosen to simulate the response of *C. littorale* to different day lengths and light intensities (the Netherlands, Norway, Brazil and Spain). Indoor experiments (simulated summer) were carried out with Original and S5, showing that S5 had a doubled TAG productivity under N-starvation. Finally, simulations of biomass and TAG productivities of Original and S5 at different locations were performed. At locations with lower light intensities, Norway and the Netherlands, biomass productivities were higher than at locations with higher light intensities, Brazil/Spain. Such results might be associated with light-saturation effects. TAG productivities, however, showed no effect of local light intensity. Locations at higher latitudes, Norway/Netherlands, cannot sustain phototrophic year-round production, hence, the yearly average TAG productivities were doubled in Brazil/Spain (from 1.4–1.6 to 3.0–3.2 g m^{-2} d^{-1}). Likewise, *C. littorale* S5 was simulated with doubled TAG productivities when compared with Original, at all locations (2.5–2.7 (low light) to 4.7–5.2 g m^{-2} d^{-1} (high light)). The present results confirm the industrial potential of *Chlorococcum littorale*, both Original and S5, as a source of TAG. Furthermore, our results can be used for comparison and to estimate future production scenarios.

1. Introduction

Microalgae have been argued to be the next feedstock for energy, food and feed in the XXI century [14]. However, microalgae have high production costs, which makes production of microalgal biomass only economic feasible, to the present date, for high-value products, e.g., pigments, and food supplements [29,41]. Therefore, reducing production costs by increasing productivities is imperative, which can be achieved with a combination of strain improvement (biology) and reactor optimization (engineering) [15,41]. Optimization experiments are, usually, costly and time consuming, two problems that can be solved using modelling techniques to simulate production scenarios.

Modelling is a powerful tool to evaluate the potential of different variables on microalgae growth and metabolism [6,11,19,36]. A few models have been developed for microalgae, mostly describing biomass productivity as a function of light intensity [1,35,36]. The limitation of these models is that they don't describe neither the concentration of intracellular components, nor the cellular response under starvation conditions. Since it is known that green microalgae accumulate carbon storage compounds under N-starvation [24,30], we require a model that describes the carbon partitioning after N-starvation (i.e., the fate of the photosynthetically absorbed energy inside the cells after nitrogen is depleted).

This carbon partitioning has been described and modelled for the green microalgae *Scenedesmus obliquus* under continuous light (both wildtype and a starchless mutant) [11]. This model can describe the dynamics between intracellular starch and TAG production rates of *Scenedesmus obliquus*, allowing estimations of productivities under different light intensities. Before applying this model to *C. littorale* we needed to validate the model, which was previously developed for

* Corresponding author.
E-mail address: iago.dominguezteles@wur.nl (I.T.D. Cabanelas).
[1] www.AlgaePARC.com

http://dx.doi.org/10.1016/j.algal.2017.08.010
Received 15 December 2016; Received in revised form 2 August 2017; Accepted 2 August 2017
Available online 17 August 2017

another strain and under different growth conditions. After validation, the model allows description of productivities of biomass components of *C. littorale* under outdoor conditions.

We evaluated the potential of two cell populations of *Chlorococcum littorale* to produce tryacilglycerols (TAG) under different climate conditions. We selected, in a previous study, a new cell population of *Chlorococcum littorale* using fluorescence activated cell sorting (FACS) [12]. This new population, namely S5, showed a stable doubled triacylglycerol (TAG) productivity in comparison with the original population due to an increased TAG content, while keeping the same growth rate.

In the current research, we first evaluated the performance *Chlorococcum littorale* (Original and S5) under simulated Dutch summer conditions (laboratory scale). Second, we used the lab scale experimental results to validate the model. Third, indoor results (and simulations) were compared with outdoor pilot-scale results (and simulations), to evaluate the ability of the model to estimate outdoor productivities. Finally, the model was applied to simulate biomass and TAG productivities of *C. littorale* (Original and S5) at four different locations, with different day lengths and light intensities (the Netherlands, Norway, Brazil and Spain).

2. Model description

A mechanistic model was previously developed for the green microalgae *Scenedesmus obliquus*. The model estimates yields and productivities of intracellular components using the carbon partitioning towards carbohydrates and lipids under N-starvation and continuous light [11]. Carbon partitioning of green microalgae refers to the fate of the photosynthetically converted photon energy into the cell. We included a day:night cycle in the model, which required adaptations to account for night biomass losses (dark respiration). Microalgae under phototrophic growth need to respire part of their biomass to provide energy for maintenance (ms) during dark periods. To validate the model for *C. littorale* (Original and S5) input biological parameters were estimated. Briefly, the input parameters are growth rate, initial biomass composition, intracellular compounds production rates and biomass degradation rate. A full list of parameters and how they were calculated can be found at Table S1 of supplementary materials. The experiments were done in flat panel photobioreactors under Dutch summer simulated conditions (Section 3.2 of methods). Fig. 1 describes the structure of the model, in which energy is first allocated to cover the maintenance requirements (ms). Once $_{ms}$ is covered two scenarios are distinguished: nitrogen is available (N+, growth phase) or not (N−, starvation phase).

Under N+ conditions the photosynthetic energy is first used to cover $_{ms}$ and is then directed to build functional biomass (X, Fig. 1). Functional biomass (X) accounts for biomass produced until nitrogen depletion, hence including nitrogen derived compounds such as proteins, aminoacids, nucleic acids and also the other biomass constituents, such as starch, TAGs and carbohydrates (non-starch). Under N− conditions the photosynthetic energy, after covering ms, is used to produce carbon derived compounds. We observed very little protein and chlorophyll degradationand during N-starvation in *Chlorococcum littorale*, such robustness has been described in our previous studies ([12], Cabanelas et al., 2016). We measured also the cellular nitrogen content (Q), which was found to be consumed during N-starvation. The mechanism described by Breuer et al. [11] defines that after a critical value of Q is reached, the cell starts to produce more TAG than starch, hence changing its metabolic response. The cellular nitrogen content (Q) is correlated to the photon partitioning (f_{TAG} Eq. (6), Supplementary materials) to derivate the biomass composition during N-starvation, i.e. how much of photon energy will be used to produce TAG or starch (STA). At the start of the N-starvation, a fixed amount of non-starch structural carbohydrates (CHO) is produced. This amount is assumed to be constant throughout the starvation period. Following, the available energy is used to produce STA and TAG. The model also accounts for conversion from STA to TAG. Additionally, STA is used as an energy source to cover maintenance during dark periods. Hence, a fraction of STA in the biomass is used for dark respiration; arrow STA → $_{ms}$ on Fig. 1. The model accounts for respiration of STA in functional biomass (X) to cover maintenance, if all STA produced under N− conditions is respired (arrow X → $_{ms}$ on Fig. 1; conditions not found in the current research).

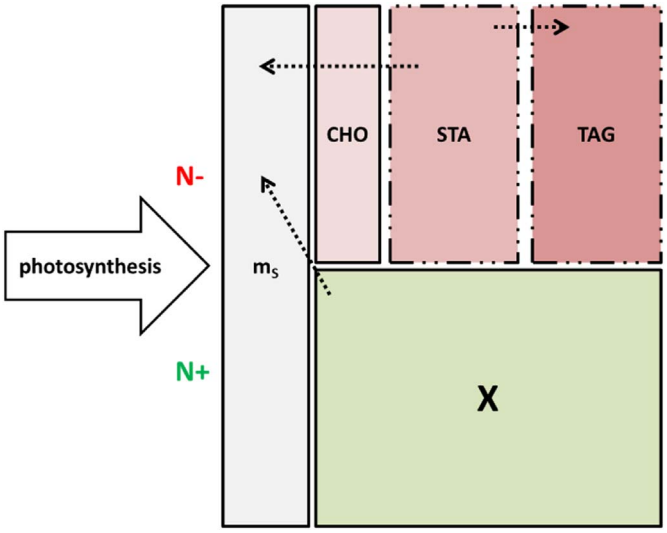

Fig. 1. Scheme of partitioning of photosynthetic energy. Regardless of the scenario, the energy from photosynthesis will first be used to cover the maintenance requirements ($_{ms}$). After maintenance is covered, two scenarios were designed in our experiments: N-replete (N+) and N-deplete (N−). The N+ scenario refers to the growth phase of our experiments, i.e., the days in which extracellular nitrogen is available. Hence, the available energy from photosynthesis (after covering $_{ms}$) will be used to produce functional biomass (i.e., biomass used for cellular proliferation). Under N− scenario, the metabolism of microalgae will change, once no N is available to sustain cellular proliferation. Hence, the available energy from photosynthesis (after covering $_{ms}$) will be used to produce 3 classes of compounds in the following order: 1] CHO (carbohydrates other than starch) will be produced and remain constant troughout the starvation phase; 2] starch (STA) and 3] triacylglicerols (TAG) will be produced as reserve compounds. Both $_{ms}$ and CHO are represented in closed boxes because they represent constant values under N-starvation. STA and TAG are represented in dotted lines because they are the dynamic compounds under N-starvation. The arrows represent the metabolic alternatives used by microalgae under N-starvation. In dark respiration, $_{ms}$ energy will be covered by starch degradation (STA → $_{ms}$). The model also describes the conditions in which starch can be converted to TAG (STA → TAG). If there is no accumulated STA available, $_{ms}$ will be then covered by the starch fraction of the functional biomass X (X → $_{ms}$), which was produced previously when N was available. The boxes are colloured according to the phase in which they belong: functional biomass (X) is only produced under N+ (green), while CHO, STA and TAG are only produced under N− (shades of red). (For interpretation of the references to colour in this figure legend, the reader is referred to the web version of this article.)

3. Materials and methods

3.1. Inoculum preparation

Two cell populations of *Chlorococcum littorale* were used: Original (NBRC 102761) and S5, which is a new cell line developed by us in a previous research ([12]). S5 was developed using cell sorting (FACS), hence selecting cells with a specific phenotype (doubled lipid productivity) to make a separate new population. The phenotype of S5 is stable 1.5 years after the selection and more details can be found in the previous publication [12]. Inocula from both populations were prepared from samples conserved in petri dishes containing growth medium (artificial seawater, as shown below) and agar (12 g l^{-1}). Homogenous aliquots from biomass were taken from petri dishes and transferred to 200 ml sterile borosilicate Erlenmeyer flasks, containing 100 ml of sterile artificial seawater medium. Artificial seawater had the

following composition ($g\,l^{-1}$): NaCl 24.55, $MgSO_4{\cdot}7H_2O$ 6.60, $MgCl_2{\cdot}6H_2O$ 5.60, $CaCl_2{\cdot}2H_2O$ 1.50, $NaNO_3$ 1.70, HEPES 11.92, $NaHCO_3$ 0.84, EDTA-Fe(III) 4.28, K_2HPO_4 0.13, KH_2PO_4 0.04. The medium also contained trace elements ($mg\,l^{-1}$): $Na_2EDTA{\cdot}2H_2O$ 0.19, $ZnSO_4{\cdot}7H_2O$ 0.022, $CoCl{\cdot}6H_2O$ 0.01, $MnCl_2{\cdot}2H_2O$ 0.148, $Na_2MoO_4{\cdot}2H_2O$ 0.06, $CuSO_4{\cdot}5H_2O$ 0.01. No HEPES was added to the medium in the experiments done with reactors (indoor and outdoor).

3.2. Experimental set-up

To compare both Original and S5 and to validate the previously developed model to *C. littorale*, simulated Dutch summer conditions were used in a lab-scale flat-panel photobioreactor. The simulated Dutch summer consisted of day length of 16 h and light supplied with a sinusoidal function with a solar noon at 1500 μmols $m^{-2}\,s^{-1}$ (resulting in an average daily incident light intensity of 636 μmols $m^{-2}\,s^{-1}$). The flat panel reactor had a working volume of 1.9 L, light path of 0.02 m, and 0.08 m^{-2} illuminated surface area (Labfors, Infors HT), reactor's details available at Breuer et al. [10]. Air flow was set at 1.0 L min^{-1} and air was mixed with CO_2, on demand, to automatically adjust pH at 7.0. Temperature was controlled with an integrated water-jacket at constant 25 °C.

The outdoor experiment was carried out with the Original in a 90 L horizontal tubular oriented reactor with a surface area of 4.6 m^{-2}, as described by Benvenuti et al., [3]. The system was inoculated to reach an initial biomass concentration of 0.4 $g\,l^{-1}$ in N-free natural seawater (same media composition as in Section 3.1). Nitrogen ($N\text{-}NO_3$) was added after inoculation to achieve the desired concentration. The reactor was sterilized via addition of 5 ppm hypochlorite before starting a run. The 2 outdoor runs were performed between August–September 2015 (with online measurements of temperature, light intensity, CO_2 and O_2 gas flow, turbidity and pH).

3.3. Daily measurements

For both indoor and outdoor experiments, samples were taken 1/2 h after sunrise and 1/2 h before sunset, which gave us the evolution of biomass and its components due to photosynthetic activity. For the outdoor experiments another extra sample in the middle of the light period, at 14:00, was also taken. For the indoor experiments we wanted to do further investigate night biomass losses, hence two samples were taken during dark periods, 2 h and then 5 h after sunset (which was feasible, since at indoor scale it was possible to invert the clock of the reactor, allowing sampling of dark samples during afternoons). For the outdoor experiments, biomass night respiration was measured with the difference between sunrise – sunset samples.

All samples were analyzed immediately after they were taken. Optical density (OD) of the algal culture was measured in a spectrophotometer (HACH, DR5000) at wavelengths of 680 nm and 750, which were proxies for chlorophyll and turbidity concentrations, respectively. Biomass production in the reactor was measured gravimetrically using GF/C Whatman filters (oven dried at 105 °C, 24 h). The Quantum Yield (QY) of photosystem II was determined in culture samples using a fluorometer (AquaPen-C AP-C 100, Photon System Instruments, Czech Republic), with the goal to assess the photosynthetic activity of cells throughout cultivation. The absorption coefficient (α) was calculated using the culture absorbance spectrum, which was determined by a fibre optic spectrometer (AvaSpec-2048, Avantes BV, Apeldoorn, Netherlands; light source: AvaLight-Hal). The measurement (in g m^{-2}), is given by Eq. (1).

$$\alpha = \frac{\sum_{400}^{700} abs_\lambda \frac{\ln(10)}{z}}{300 \bullet c_{DW}} \quad (1)$$

with z: light path of the precision cellc_{DW}: dry weight of the sample

Extracellular nitrogen content ($N\text{-}NO_3$, $mg\,l^{-1}$) was measured using samples of 1 ml algae suspension. Samples were centrifuged for 5 min at 13300 rpm (Micro Star 17R, VWR®) and the supernatant immediately measured with a nutrient analyzer (AQ2, SEAL Analytical Inc., USA) according to the NO_3 method by SEAL-Analytica.

3.4. Biomass analyses

The intracellular nitrogen concentration was determined from freeze-dried biomass samples via combustion followed by chromatography (Flash EA 2000 elemental analyzer, ThermoFisher Scientific, USA). For analyses of biomass composition (expressed in g g DW^{-1}) freshly harvested samples were centrifuged twice and washed with MilliQ water (3134 g for 10 min at 4 °C) and followed by freezing at − 20 °C and freeze-drying for 24 h. Triacylglycerols (TAGs) and polar lipids were extracted from the same samples and quantified using GC/MS column chromatography, as described by Breuer et al. [9]. Total carbohydrates were analyzed with the phenol-sulfuric acid method developed by Dubois et al., [17]. Total starch was analyzed with the colorimetric/enzymatic method from the commercial kit from Megazyme (K-STA kit, UK).

3.5. Calculations

The following calculations were not used as model input, but they were used to compare the results of experimental data (indoor and outdoor) with each other. Time intervals are indicated in the description of each equation to assist interpretation.

The specific growth rate (Eq. (2)) was calculated as the change in biomass concentration (expressed as natural logarithm) as a function of time from inoculation until nitrogen starvation. Where: DW is dry weight of biomass ($g\,l^{-1}$), $t_{=0}$ stands for the start of the cultivation, while $t_{N=0}$ stands for the time in which $N\text{-}NO_3$ equals zero.

$$\mu = \frac{\ln(DW_{N=0} - DW_{t_0})}{t_{N=0} - t_0} \quad (2)$$

Biomass productivity (P_{Cx}, Eq. (3)) during growth phase was calculated as the change in biomass concentration ($g\,l^{-1}$) between inoculation and nitrogen starvation. Where: DW is dry weight of biomass ($g\,l^{-1}$), $t_{=0}$ stands for the start of the cultivation, while $t_{N=0}$ stands for the time in which $N\text{-}NO_3$ equals zero.

$$P_{cx} = \frac{DW_{N=0} - DW_{t_0}}{t_{N=0} - t_0} \quad (3)$$

Average night Biomass Loss ($NBL_{,ave.}$ in $g_{Cx}\,L^{-1}$ night) was calculated as the difference of measured biomass ($g\,l^{-1}$) before and after each night period, followed by averaging over the nitrogen starvation cultivation period. Average starch night respiration ($SNR_{,ave}$) was calculated in the same way but using the starch concentration instead of biomass concentration.

Average TAG productivity (Eq. (4)) was calculated as the change in TAG concentration ($g\ l^{-1}$) for the total N-starvation period (period indicated at Tables 1 and 2). Where: TAG stands for TAG concentration ($g\,l^{-1}$), the time frames $N = 0$ indicates the start of the N-starvation period and t = f the end of the N-starvation period (end of cultivations).

$$P_{TAG,avg} = \frac{TAG_f - TAG_{N=0}}{t_f - t_{N=0}} \quad (4)$$

The maximum time average TAG productivity ($P_{TAG,max}$, $g\,l^{-1}\,d^{-1}$) was calculated according to Eq. (4), with the exception that only the period from N-starvation ($N = 0$) to the highest TAG productivity was accounted (Original and S5 [both indoor]: day 2 to 4; Outdoor: day 3 to 6).

Maximum areal time average ($P_{TAG,max,areal}$, $g\,m^{-2}\,d^{-1}$) was calculated by multiplying the $P_{TAG,max}$ by the illuminated surface area of the reactors (0.08 m^{-2} for indoor and 4.6 m^{-2} for outdoor). For the

Table 1
Overview of growth parameters, biomass and TAG productivities, yields of biomass and TAG on photons for indoor experiments with Original and S5 under simulated Dutch summer conditions, and of outdoor experiment with Original. Results are derived from 2 biological replicates. Standard deviations were not shown because all were below 5% variation from the mean, with the exception of starch for outdoors (13%).

	Unit	Time frame	Indoor (Original)	Indoor (S5)	Outdoor (Original)
PFD	mol m^{-2} d^{-1}		55.0	55.0	30.1
Biomass production (Cx)	g_{Cx} L^{-1}	Final day	4.65	7.71	4.28
Growth rate (μ)	d^{-1}	$t_0 - t_{N=0}$	0.69	0.72	0.45
Biomass productivity (Px)	g_{Cx} L^{-1} d^{-1}	$t_0 - t_{N=0}$	1.04	1.09	0.64
Biomass areal productivity ($P_{X, area}$)	g_{Cx} m^{-2} d^{-1}	$t_0 - t_{N=0}$	23.4	24.5	12.5
Biomass yield ($Y_{cx,ph}$)	g_{Cx} mol^{-1}	$t_0 - t_{N=0}$	0.43	0.45	0.42
Night biomass losses, average (NBL_{ave})	g_{Cx} L^{-1} $night^{-1}$	N-starvation period	0.25	0.23	0.42
Starch night respiration ($SNR_{,ave}$)	g^{-1}_{STA} L^{-1} $night^{-1}$	N-starvation period	0.20	0.23	0.19
TAG average productivity ($P_{TAG,ave}$)	g L^{-1} d^{-1}	N-starvation period	0.17	0.32	0.08
Max time average TAG productivity $P_{TAG\ max\ time\ ave}$	g L^{-1} d^{-1}	48h after start of N-starvation (indoor), between t=3 to t=6 (outdoor)	0.21	0.4	0.14
TAG yield ($Y_{TAG,ph}$) Max time average	g_{TAG} mol^{-1}		0.09	0.16	0.09
TAG areal productivity, maximum time average ($P_{TAG,area,\ max,\ ave}$)	g_{TAG} m^{-2} d^{-1}		4.72	9.00	2.74
TAG	g g^{-1}_{Cx}	End of N-starvation	0.21	0.30	0.15
STA	g g^{-1}_{Cx}	End of N-starvation	0.25	0.29	0.18
CHO	g g^{-1}_{Cx}	End of N-starvation	0.20	0.19	0.28

The color in the table relate to the physiologic state of the cultures. Green color mark the parameters derived from the growth phase (as it can be seen in the green areas marked in Figs. 2 and 3). The yellowish color is to highlight the N-starvation phase.

indoor flat panels the illuminated surface refers to the area of the panel receiving light form one side (no loss is assumed since the reactor is covered to avoid light going out or in). For the outdoor systems, we considered the ground area of the tubular PBR, considering that the calculated light is measured as total amount of photons impinging on the surface (the space between tubes was neglected, as was calculated by Benvenuti et al. [3] and de Vree et al. [16]).

Yearly areal TAG productivity ($P_{TAG,yearly,areal,}$ $g\ m^{-2}\ y^{-1}$) was calculated by multiplying $P_{TAG,max}$ by the total amount of production days per year for each simulated locations: 150 days for Oslo, Norway/Wageningen,the Netherlands; and 300 for Rio, Brazil/Cádiz, Spain.

Yearly average areal daily productivity ($PTAG_{,ave.,daily,\ areal,}$ $g\ m^{-2}\ d^{-1}$) was calculated dividing the $P_{TAG,yearly,areal}$ for each location by the number of days per year (365), hence normalizing the productivities.

Biomass and TAG yields on light ($g\ mol^{-1}$) were calculated by division of the respective productivities (Eqs. (2) and (3)) by the corresponding total amount of light impinging on the reactor surface (indicated in Tables 1 and 2).

3.6. Data analyses

The sample standard deviation (SD) was calculated between the biological replicates (a least 3) for every estimated parameter. The estimated SDs were used to show the data variability between biological replicates for productivities and kinetic parameters (Table 1). The standard deviations were also used to estimate the 95% confidence intervals (with a two-tailed T-distribution) for every experimentally estimated parameter used to run model simulations (supplementary materials, Table S1). These calculations were carried out with Microsoft Excel 2010.

The confidence intervals (as stated above) were used to evaluate goodness of fit between experimentally measured values and simulated values. As a result, the dot plots between experimentally measured values and simulated values show the upper and lower confidence intervals. This analysis was carried out with MATLAB R2015a (© 2016 The MathWorks, Inc.).

Table 2
Simulated of growth parameters, biomass and TAG productivities, yields of biomass and TAG on photons for both Original and S5, at four different locations worldwide. Yearly daily TAG productivity was calculated multiplying the maximal areal productivity (PTAG, yearly average areal productivity, g m^{-2} d^{-1}) by the amount of production days and further dividing by the days of the year (150 production days at Norway/Netherlands and 300 days at Rio/Cádiz); for all cases the final result was divided by 365, thus normalizing the measurement.

		Oslo (Norway)		Wageningen (the Netherlands)		Rio de Janeiro (Brazil)		Cadiz (Spain)	
Parameters	**Units**	**Original**	**S5**	**Original**	**S5**	**Original**	**S5**	**Original**	**S5**
day length	h	16.45		15.17		11.98		12.03	
Photon flux density (PFD)	mol $m^{-2}d^{-1}$	31.51		33.07		37.77		41.83	
Growth phase	days	1.69	1.79	1.64	1.81	2.41	2.4	2.41	2.4
Growth rate (μ)	d^{-1}	0.62	0.53	0.61	0.5	0.46	0.46	0.47	0.46
Biomass productivity (P_{Cx})	g_{Cx} $l^{-1}d^{-1}$	0.74	0.71	0.7	0.64	0.58	0.67	0.6	0.67
Biomass areal productivity ($P_{Cx,areal}$)	g_{Cx} $m^{-2}d^{-1}$	16.6	15.9	15.7	14.4	13.05	15.08	13.5	15.08
Biomass $yield_{Cx}$ (Y_{Cx})	g_{Cx} mol^{-1}	0.53	0.51	0.48	0.44	0.34	0.4	0.32	0.36
P_{TAG}, ave (From t_2 to t_f)	g $l^{-1}d^{-1}$	0.11	0.17	0.12	0.17	0.14	0.18	0.14	0.18
P_{TAG}, max time ave (From t_2 to t_4)	g $l^{-1}d^{-1}$	0.14	0.22	0.15	0.22	0.17	0.23	0.18	0.23
TAG yield, max time ave ($Yield_{TAG}$)	g $l^{-1}d^{-1}$	0.1	0.15	0.1	0.15	0.1	0.13	0.1	0.12
P_{TAG},max areal time ave	g $m^{-2}d^{-1}$	3.15	4.95	3.38	4.95	3.83	5.18	4.05	5.18
$P_{TAG,\ yearly\ area}$	g $m^{-2}y^{-1}$	473	743	506	743	1148	1553	1215	1553
P_{TAG}, Yearly average areal daily productivity	g $m^{-2}d^{-1}$	1.29	2.03	1.39	2.03	3.14	4.25	3.33	4.25

3.7. Outdoor climate data

Four different locations were chosen to simulate the potential of both *C. littorale* Original and S5, i.e., Wageningen (the Netherlands), Oslo (Norway), Rio de Janeiro (Brazil) and Cádiz (Spain). These locations were chosen to simulate the response of *C. littorale* to different day lengths and light intensities. Locations at higher latitudes, Norway and the Netherlands, cannot sustain year-round phototrophic microalgae production. Hence, for Norway and the Netherlands cultivation periods from April to September were considered. The yearly average light intensity and day length for each location were estimated and are presented in Table 2 and Fig. 4.

The solar radiation data was derived from the HelioClim radiation Databases of SoDa (www.soda-is.com), which estimates total solar irradiance and irradiation values at ground level from Meteosat Second Generation (MSG) satellite images [31]. Data from light on a horizontal

plane (global radiation), day length and different measurement intervals (5 min, hourly, weekly and monthly) were included. The conversion from Irradiance (W/m^2) to PAR ($\mu mol/m^2/s$) was calculated manually according to [27] (factor of 2.3). Monthly data of the last 15 years were averaged to provide a realistic irradiance value to be used as model input.

Cultivation periods from April to September were assumed for the Netherlands and Norway, because this is the period with the highest light intensity. These light intentisities are assumed to sustain biomass productivity. For Rio and Cádiz all year round cultivations were considered. Cultivations were assumed to be done in a flat panel photobioreactor, similar to the one described in the methods (3.2). The input parameters, day length and light intensity, were derived from the average of all months during this period. The model is loaded with the light intensity (I; $\mu mol\ m^2\ s^{-1}$) and the day length for each location. Hence, to estimate daily total irradiance (photon flux density, PFD; $mol\ m^{-2}\ d^{-1}$), the following equation was used:

$$PFD = I*86400/1000000 \quad (5)$$

where 86,400 is the factor to convert the light intensity (I) from seconds to days, and 1,000,000 is the factor to convert the values from μmol to mol.

4. Results and discussion

4.1. Comparing indoor and simulated performances of original and S5

Indoor experiments were carried out with Original and S5 to compare the performance of both populations. Secondly, the experiments were used to derive the biological parameters necessary to model the productivities. Original and S5 were cultivated in a N-runout batch, which means that functional biomass was produced up to the time point at which N was depleted from the growth medium (green area, Fig. 2). Both growth rate and biomass productivity showed no differences between Original and S5 in this period (Table 1). After all nitrogen was consumed by the cells (green area, Fig. 2), starch and TAG were produced as a known biological response of microalgae to N-starvation [25,40]. During N-starvation, S5 showed an increased biomass accumulation in comparison with Original (maximum biomass concentration 7.7 $g\ l^{-1}$ against 4.6 $g\ l^{-1}$ from Original, Table 1), which was accounted for an increased TAG content (0.30 $g\ g^{-1}$ against 0.21 $g\ g^{-1}$ from Original, Table 1).

Table 1 also provides a comparison of TAG productivities and yields between Original and S5. The average TAG productivity ($P_{TAG,ave}$), which considers the entire N-starvation period of 7 days was 1.9 × higher in S5 in comparison with Original. The maximum time average productivity ($P_{TAGmax,time,ave}$) is calculated considering only the period of starvation in which maximum TAG daily productivity takes place. For both Original and S5 the $P_{TAGmax,time,ave.}$ was measured 48 h after N-starvation, confirming a 1.9 × higher performance by S5 (Table 1). These results showed the industrial potential of S5 for TAG production, since this cell population has been developed 1.5 years before the current experiments, highlighting a stable phenotype [12].

The experimental data presented above were used to calculate the necessary input parameters for the model simulations. The mechanistic model [11] had to be validated for *C. littorale* under simulated Dutch summer conditions, as it was originally developed for *S. obliquus* under continuous light. The model was modified to include a day night cycle, which requires inclusion of dark respiration (night biomass losses, NBL). Dark respiration means that part of the biomass that was produced during the day is used during dark periods to cover maintenance [18,37]. Average night biomass losses (NBL_{ave}) were calculated for Original and S5 accounting the whole period of N-starvation. Both Original and S5 showed similar rates of NBL_{ave} (0.25 and 0.23 $g_{Cx}\ L^{-1}\ night^{-1}$ respectively, Table 1). According to experimental data only starch is degraded during night to cover maintenance requirements of both Original and S5 (and simulated data follows closely). This conclusion can be derived from the average starch night respiration (SNR), which presented similar values and the NBL (0.20 $g_{STA} l^{-1}\ night^{-1}$ for Original and 0.23 $g_{STA}\ l^{-1}\ night^{-1}$ for S5, Table 1).

The modelled data generally followed the trends of the experimental data (concentrations of biomass, TAG and starch, $g\ l^{-1}$, Fig. 2). Extracellular nitrogen concentration ($mg\ l^{-1}$) was accurately simulated, since both experimental and modelled mark the start of the N-depletion phase at the same time point (green area, Fig. 3). For both Original and S5 simulated biomass concentration is underestimated during N-starvation, which can be related to the underestimation of TAG concentrations also during the N-starvation phase (Fig. 2). Starch concentrations, however, followed closely the experimental data including the night respiration of biomass (Fig. 2). Additionally, the confidence intervals (CI) between simulated and experimentally measured data were calculated for biomass, TAG and STA concentrations (both Original and S5; Figs. S2–4, supplementary materials). For all parameters almost all data points fell within the confidence intervals, with biomass and TAG concentrations showing higher accuracy than starch.

Chlorococcum littorale consumes only starch during night respiration to cover maintenance requirements, which is understandable considering the higher energy yield (on ATP) of starch in comparison with TAGs [23]. Such results have industrial implications when aiming to produce TAGs from *C. littorale* since no TAG respiration was observed in the current research, indicating the potential of both Original and S5 for TAG production under real light conditions. *C. littorale* Original is already among the most productive strains in the literature, for both biomass and TAG [20,28,32]. Recent studies register an areal TAG productivity of *Nannochloropsis* sp. (one of the most studied strains for TAG production) between 2.0 and 6.5 $g_{TAG}\ m^{-2}\ d^{-1}$, considering indoor and outdoor experiments ([2–4]; Paolo [7,32,33]). *C. littorale* S5 showed the same biomass productivity as Original, but a 2-fold increased TAG productivity (S5: 9.0 g against Original: 4.7 $g_{TAG}\ m^{-2}\ d^{-1}$). The doubled TAG productivity of S5 makes it competitive for TAG production. In summary, we conclude that the model was validated for *C. littorale* using experiments under simulated summer conditions, which gives the possibility to estimate the performance under outdoor conditions. We also highlight that *Chlorococcum littorale* S5 showed indoor TAG productivities above the values reported for the most productive strain in the literature. Furthermore, the results in biomass and TAG productivities from the simulations indicate the potential of S5 to be produced at industrial scale.

4.2. Comparing simulations from indoor to outdoor

Results of the outdoor run with the wildtype of *Chlorococcum littorale* were used to estimate the parameters required to run simulations of biomass, TAG and starch concentrations (Fig. 3). In Fig. 3 it is possible to see that, like the indoor experiments, the simulated data for the outdoor run also generally followed the experimental data. Differently from the indoor experiments, under outdoor conditions the amount of light available varies on a daily basis, causing a variability to the data set. Both biomass and TAG concentrations showed acceptable confidence intervals, while starch showed much higher intervals (Fig. S1-S3, sup materials). These results are nevertheless remarkable considering that the model simulated a flat panel (2 cm depth reactor), while the outdoor experiments were carried out in a tubular pilot reactor (tubes diameter 0.05 m). One explanation could be that the combination of biomass concentration and light intensity outdoors were close to the optimum for *C. littorale*. The biomass concentration in the outdoor experiments was chosen considering the indoor experiments, to keep both experimental conditions comparable.

Chlorococcum littorale, in outdoor experiments, required twice the time (3 days, compared with 1.7 from indoor) to consume all extracellular nitrogen when compared with indoor experiments (i.e., growth

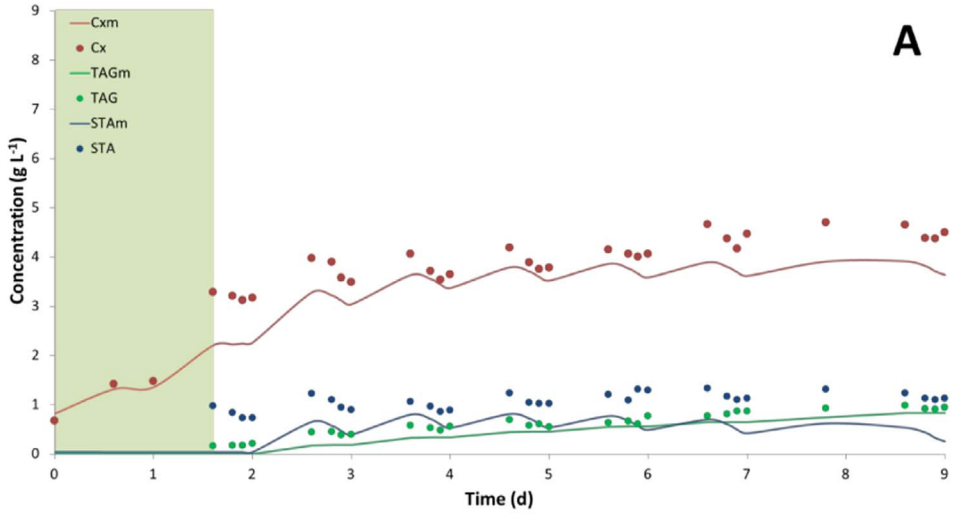

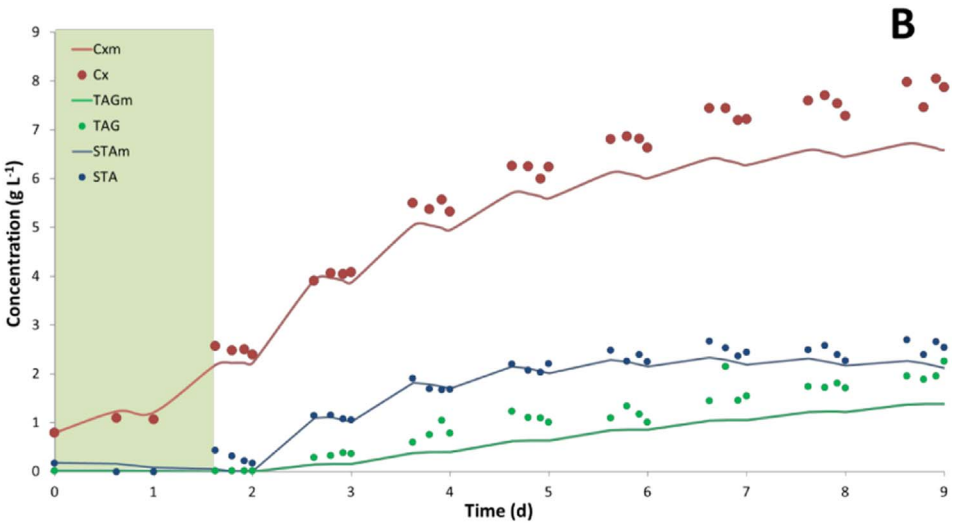

Fig. 2. Results from indoor experiments. Concentration of biomass (Cx), starch (STA) and triacylglycerides (TAG) for both original (A) and S5 (B). Symbols represent the experimentally obtained values, while the lines represent model simulation results. The green area represents the period of the cultivation in which nitrogen was available, i.e., the growth phase (N + phase). From day 1.7 onward it is considered as nitrogen starvation phase (N-starvation). (For interpretation of the references to colour in this figure legend, the reader is referred to the web version of this article.)

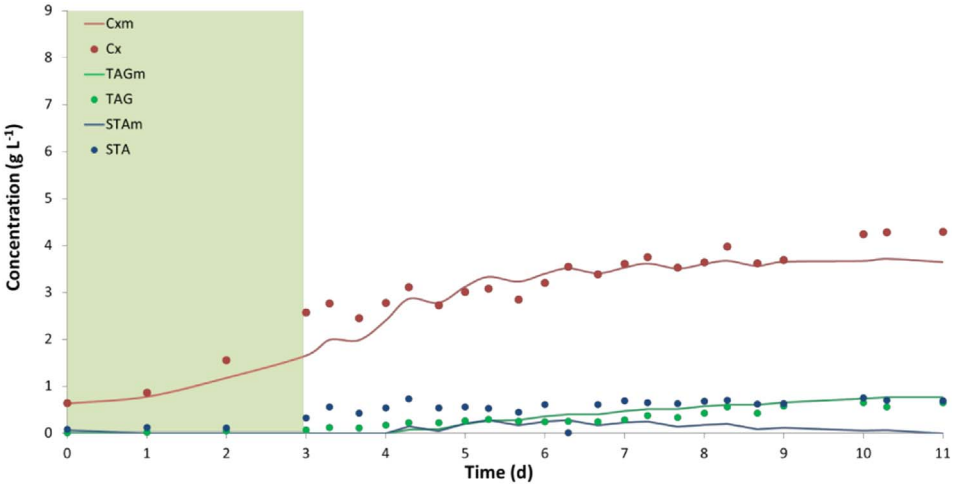

Fig. 3. Concentration of biomass (Cx), starch (STA) and triacylglycerides (TAG) for the outdoor experiments with Original. Symbols represent the experimentally obtained values, while the lines represent model simulations. The green area represents the period of the cultivation in which nitrogen was available, i.e., the growth phase (N + phase). From day 3 onward it is considered nitrogen starvation phase (N − phase). (For interpretation of the references to colour in this figure legend, the reader is referred to the web version of this article.)

phase, N + phase, Fig. 3). This resulted in a lower growth rate when compared with indoor experiments (from 0.69 d^{-1} indoor to 0.45 d^{-1} outdoor). The same interval (day 0 to day 3) was used to estimate the average biomass productivity outdoors, which was lower than under indoor conditions (0.64 against 1.04 $g\,l^{-1}\,d^{-1}$, Table 1). Such results were expected due to a lower light intensity outdoors (30 against 55 $mol\,m^{-2}\,d^{-1}$, Table 1). The same applies for TAG productivity, which was 0.14 $g\,l^{-1}\,d^{-1}$ outdoor, against 0.21 $g\,l^{-1}\,d^{-1}$ indoor ($P_{TAGmax,time,ave.}$, Table 1). However, when comparing yields on light energy (g biomass/TAG per mol light), the values were the same. The comparison of the yields was done using the equivalent time intervals, which confirms that the biological functions responded similarly during indoor and outdoor cultivation.

Average night biomass losses (NBL_{ave}) under outdoor conditions

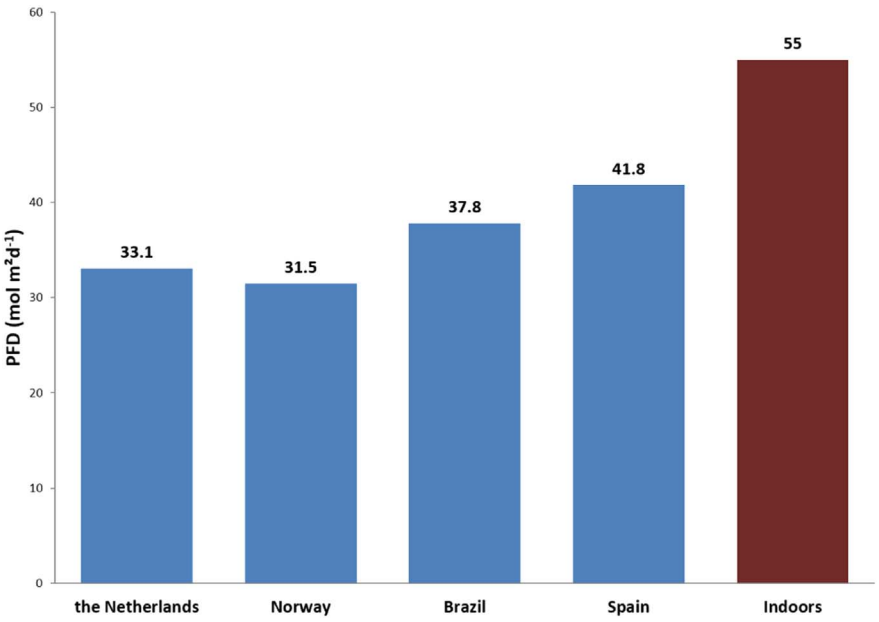

Fig. 4. Photon flux density (PFD, mol $m^{-2} d^{-1}$ for the Netherlands, Norway, Brazil and Spain; as well as for the indoor experiments simulating a Dutch summer day). The values from Norway and the Netherlands are averages for the cultivation period from April to September, while average values of PFD for the whole year are shown for Rio and Cádiz. Details on the acquisition and calculation of light intensities are available in Materials and methods. The different periods of production for Norway/Netherlands impacted the year-round productivities, because the number of production days was 150/year, while for Brazil/Spain it was 300/year.

were higher than under indoor conditions (0.42 against 0.23 $g_{Cx} l^{-1}$ night^{-1}, Table 1). Differently from indoor, under outdoor conditions the NBL_{ave} could not be solely attributed to starch degradation (0.19 $g_{STA} l^{-1}$ night^{-1}, Table 1) and neither to any of the other analyzed biomass components (carbohydrates, TAGs and polar lipids all showed no night degradation). Additionally, lower biomass concentrations were achieved outdoors (4.28 against 4.65 $g_{Cx} l^{-1}$ indoors, Table 1). Hence, it can be hypothesized that part of the produced biomass (whole cells) is respired under outdoor conditions. The higher maintenance determined outdoor in comparison with indoor also corroborates this finding (Table S1, sup materials). The higher outdoor maintenance ($_{ms}$) could be a consequence of more dark zones in the horizontal tubular reactor when compared with the flat panel (indoor). The reactor used in the outdoor experiments was a horizontal tubular reactor with 0.05 m diameter tubes (section Experimental set-up, Materials and methods), different from the 0.02 m light path flat panel reactor used for the indoor experiments. This difference in design, from a narrow flatpanel to a tubular reactor, can explain the higher respiration rate, which can explain the increase in the measured maintenance ($_{ms}$) [36,38].In the flat panel (indoor) there are no dark zones because the small surface of the flatpanel is always completelly illuminated by a panel of LED lamps. Hence, the cells are always illuminated during the photoperiod. In the tubular reactor (outdoor) there are dark zones (corners and the degasser), which might cause some photorespiration and a lower productivity, leading to a higher $_{ms}$.

An important factor that the model does not incorporate is the influence of temperature. The outdoor runs were carried out in a system with temperature control, but that showed limited capacity during peaks of high light intensity days with high temperature. Maximum temperatures of 32 °C with an average 6–9 h above 30 °C each day (data not shown) have been reached. Chihara et al. [13] reported sub-optimal temperature above 28 °C for *C. littorale*, which might have had a negative impact on biomass and TAG yields in the present study. This is a possible explanation for the model underestimation of the biomass production. The effect of temperature fluctuation during the day was excluded in the model, i.e., the model assumes no effect of temperature on the biological response. This approach was chosen since the temperature was controlled to the optimum temperature in the indoor experiments.

The simulated productivities under outdoor conditions are in the range of what has been registered for other strains and other climate conditions. In the current research, the maximum time-averaged TAG yield reached in outdoor experiments with *C. littorale* was 0.09 g_{TAG} mol^{-1} photons. The maximum TAG yields reported by Benvenuti et al. [2–4] with *Nannochloropsis* sp. cultivated in the same horizontal tubular reactors and using the same strategy (nitrogen runout batch) as in this work, were 0.06–0.09 g_{TAG} mol^{-1} photons (depending on initial biomass concentration). Similarly, another research with *Nannochloropsis* sp. also registered a outdoor TAG yield on light of 0.06 g_{TAG} mol^{-1} photons [7,8], hence in the same range as registered for the strains used in the current study. These results highlight the industrial potential of *Chlorococcum littorale*, as it sustains similar yields as the most commonly used strain in the literature. The doubled TAG productivity of S5 indicates the potential of this cell population to outcompete the most productive strains available.

The mechanistic model was validated for *C. littorale*, Original and S5 under indoor conditions. Simulations of indoor experiments followed closely the measured data, although with biomass and TAG slightly underestimated. The simulations of the outdoor experiments followed similar trends as the experimental data despite limitations to calibrate this model to different reactor design. The results are yet remarkable, considering the differences of reactor design between indoor and outdoor experiments. The biomass concentration during outdoor experiments was chosen to keep both experimental conditions comparable, which guaranteed that the described biological parameters could be used to simulate production. Further implementation of light use, correcting for the reflection angles on the surface of tubular reactors, could make the prediction of outdoor data more accurate in the future [35]. The yields of biomass and TAG on light, however, were similar for the indoor and outdoor experiments highlighting that the biological mechanism for biomass and TAG production were similar. This finding indicates the potential of the model validated with indoor simulations to estimate outdoor performance.

4.3. *C. littorale* productivities under different locations

After validation of the model for simulations on *C. littorale*, the potential for cultivation under different light regimes was tested. Hence, the biological parameters and growth conditions from indoor experiments were used to simulate the productivities of both Original and S5. The biological parameters were combined with the light values (light intensity and day length) at 4 different locations: Wageningen (the Netherlands), Oslo (Norway), Rio de Janeiro (Brazil) and Cádiz (Spain).

The simulations considered the average total daily light impinging on ground area and the duration of the day to simulate batch N-runout cultivations of *C. littorale* Original and S5. Fig. 4 shows the average light intensity for each location (photon flux density, PFD; mol $m^{-2} d^{-1}$), in comparison with the indoor experiments. In Fig. 4 the number of running months per year is also depicted, showing that while Cádiz and Rio de Janeiro can sustain year-round phototrophic microalgae production, Norway and the Netherlands were assumed to run phototrophic production from April until September (the most sunny months). Accumulation of TAG and starch after nitrogen depletion depend on photosynthesis rate at each location. Hence, the yields of both biomass and TAG are solely dependent on light intensity and duration of the day.

Table 2 summarizes the results of the simulations of biomass and TAG productivities at different locations. At locations with lower light intensities, Norway and Netherlands, growth rates (μ) and biomass productivities (P_{Cx}) were higher (μ = 0.6 and P_{Cx} = 0.70–0.74 $g_{Cx} l^{-1} d^{-1}$) than at locations with higher light intensities, Rio de Janeiro and Cádiz (μ = 0.46 and P_{Cx} = 0.58–0.60 $g_{Cx} l^{-1} d^{-1}$). Such results might be associated with light-saturation effects, since most marine algae saturate at the peak hours of light intensity during the day, hence just a fraction of received irradiance is actually utilized for photosynthesis [21,38,39]. Additionally, Kurano & Miyachi [26] observed light saturation for *C. littorale* at light intensities above 300 μmol $m^{-2} s^{-1}$, which might explain why large increases in irradiance did not lead to increase in biomass productivities. This assumption can be corroborated by comparing biomass yields on light of *C. littorale* Original between simulations and the outdoor experiments carried out in the Netherlands (Table 1). This comparison shows that for Norway/Netherlands slightly higher biomass yields were observed (0.42 $g_{Cx} mol^{-1}$ outdoor experiment (Original, Table 1), 0.48/0.53 $g_{Cx} mol^{-1}$ for Norway/Netherlands, Table 2), than for Cádiz/Rio (0.32/0.36 $g_{Cx} mol^{-1}$, Table 2). The same trend was observed when comparing outdoor data from the Netherlands with the simulations for *C. littorale* S5.

TAG productivities showed a different trend when compared with biomass productivities, for both Original and S5. No effect of local light intensity was observed on TAG productivity or yield (Table 2). This result makes sense since the light intensities used for the simulations at all locations are all below what has been experimentally used in the current research (Fig. 4). Additionally, the amount of light used in indoor experiments didn't show any measurable negative effect during N-starvation, since no negative yield was observed during N-starvation. Some algae strains show a considerable reduction in photosynthetic activity during N-starvation, but *C. littorale* has been chosen for the current research exactly for its resilience under N-starvation [2,22]. Furthermore, we would like to highlight that the yields simulated for other climate conditions (Table 2) are similar to the yields calculated for indoor experiments (both Original and S5, Table 1) and also for the outdoor experiment (for Original only, Table 1). Simulated TAG areal productivities (P_{TAG}, max areal time ave., Table 2) under different locations were between 3.1 and 4.0 $g_{TAG} m^{-2} d^{-1}$ for Original and between 4.9 and 5.2 $g_{TAG} m^{-2} d^{-1}$ for S5. Such values are in the same order as the values reported for the genus *Nannochloropsis* (2.0 to 5.2 $g_{TAG} m^{-2} d^{-1}$) under indoor and outdoor conditions [5,7,32,33]. The same research also reports no effect of different total irradiance (outdoor) on lipid yields [3]. Hence, for biomass production of *Chlorococcum littorale* photo-saturation might reduce the yields of biomass on photons under higher light intensities. On the other hand, for TAG accumulation such an effect might not be seen, as long as light intensity is kept below the threshold of photo-damage.

Although no differences were observed among the simulated TAG productivities under different locations, attention should be paid when extrapolating the results to year-round projections. We reported the yearly average TAG productivities, which were calculated by multiplying the daily areal productivity by the number of running days per year (150 for Norway/Netherlands and 300 for Rio/Cádiz). Since the locations have different production periods, the yearly average TAG productivities were normalized by the number of days per year, allowing comparison. Yearly average TAG productivities of 1.4–1.6 $g m^{-2} d^{-1}$ were simulated for *C. littorale* Original at Norway/Netherlands, and 3.0–3.2 $g m^{-2} d^{-1}$ were simulated at Rio/Cádiz, hence doubling the year-round production. Likewise, *C. littorale* S5 was simulated with increased TAG productivities at all locations, increasing to 2.5–2.7 $g m^{-2} d^{-1}$ at Norway/Netherlands and to 4.7–5.2 $g m^{-2} d^{-1}$ at Rio/Cádiz. Locations at higher latitudes (e.g., the Netherlands and Norway) can sustain microalgae phototrophic production during spring and summer, but not year-round production. We demonstrated that *C. littorale*, Original and S5, are competitive strains to produce biomass at large scale, competing with commonly used strains. S5, however, showed similar TAG productivities as *Nannochloropsis sp.*, with the potential to outcompete it. In summary, we believe that the estimated productivities can be used for comparison purposes and for future production scenarios.

5. Conclusions

We validated a model to predict biomass and TAG productivities of *Chlorococcum littorale* under summer conditions. The validation was done for *C. littorale* Original strain and for S5, a selected cell population with doubled TAG productivity. The simulations of outdoor experiments (with Original) followed the experimental data and the yields of biomass and TAG were similar to indoor experiments. Therefore, the model can be used to estimate biomass and TAG productivities under different climate conditions. Simulations of productivities under different locations showed that biomass yield was higher at locations with lower light intensity. TAG yields, however, showed no effect of local light intensity. Yearly average TAG productivities were estimated as 1.4–1.6 $g m^{-2} d^{-1}$ for *C. littorale* Original at Norway/Netherlands, and 3.0–3.2 $g m^{-2} d^{-1}$ at Brazil/Spain. *C. littorale* S5 was simulated with increased TAG productivities at all locations, increasing to 2.5–2.7 $g m^{-2} d^{-1}$ at Norway/Netherlands and to 4.7–5.2 $g m^{-2} d^{-1}$ at Brazil/Spain. We demonstrated that *C. littorale*, Original and S5, are competitive strains to produce biomass at large scale, competing with commonly used strains. S5, however, showed similar TAG productivities as *Nannochloropsis sp.*, with the potential to outcompete it. In summary, we believe that the provided productivities can be used for comparison purposes and to estimate future production scenarios.

Acknowledgements

The authors would like to thank the financial support to AlgaePARC Research Program (TRCDKI/2010/0956). provided by: Ministry of Economic Affairs, Agriculture and Innovation (the Netherlands), Province of Gelderland (the Netherlands), and the companies: BASF, BioOils, Drie Wilgen Development, DSM, Exxon Mobil, GEA Westfalia Separator, Heliae, Neste, Nijhuis, Paques, Cellulac, Proviron, Roquette, SABIC, Simris Alg, Staatsolie Suriname, Synthetic Genomics, TOTAL and Unilever. Also, the National Council of Science and Technology (Brazil) is acknowledged for the grant 236614/2012-6. The authors also thank the support of Kira Schediwy in the early stages of this project.

Author contributions

All authors have contributed to the manuscript. All authors contributed for the research design, data analyses, and all authors have read the final version of the manuscript, hence giving feedback on the content. The experimental work was done by Iago TD Cabanelas and Hanna Bopple.

Appendix A. Supplementary data

Supplementary data to this article can be found online at http://dx.doi.org/10.1016/j.algal.2017.08.010.

References

[1] D. Baquerisse, S. Nouals, A. Isambert, P.F. dos Santos, G. Durand, Modelling of a continuous pilot photobioreactor for microalgae production, Prog. Ind. Microbiol. 35 (1999) 335–342, http://dx.doi.org/10.1016/S0079-6352(99)80125-8.

[2] G. Benvenuti, R. Bosma, M. Cuaresma, M. Janssen, M.J. Barbosa, R.H. Wijffels, Selecting microalgae with high lipid productivity and photosynthetic activity under nitrogen starvation, J. Appl. Phycol. 27 (2015) 1425–1431, http://dx.doi.org/10.1007/s10811-014-0470-8.

[3] G. Benvenuti, R. Bosma, F. Ji, P.P. Lamers, M.J. Barbosa, R. Wijffels, Batch and repeated-bacth microalgal TAG production in lab-scale and outdoor photobioreactors, October (2015), http://dx.doi.org/10.1007/s10811-016-0897-1.

[4] G. Benvenuti, R. Bosma, A.J. Klok, F. Ji, P.P. Lamers, M.J. Barbosa, R.H. Wijffels, Microalgal triacylglycerides production in outdoor batch-operated tubular PBRs, Biotechnol. Biofuels 8 (2015) 100, http://dx.doi.org/10.1186/s13068-015-0283-2.

[5] G. Benvenuti, P.P. Lamers, G. Breuer, R. Bosma, A. Cerar, R.H. Wijffels, M.J. Barbosa, Microalgal TAG production strategies: why batch beats repeated-batch, Biotechnol. Biofuels 9 (2016) 64, http://dx.doi.org/10.1186/s13068-016-0475-4.

[6] O. Bernard, Hurdles and challenges for modelling and control of microalgae for CO2 mitigation and biofuel production, J. Process Control 21 (2011) 1378–1389, http://dx.doi.org/10.1016/j.jprocont.2011.07.012.

[7] P. Bondioli, L. Della Bella, G. Rivolta, G. Chini Zittelli, N. Bassi, L. Rodolfi, D. Casini, M. Prussi, D. Chiaramonti, M.R. Tredici, Oil production by the marine microalgae *Nannochloropsis* sp. F & M-M24 and *Tetraselmis suecica* F & M-M33, Bioresour. Technol. 114 (2012) 567–572, http://dx.doi.org/10.1016/j.biortech.2012.02.123.

[8] P. Bondioli, L. Della Bella, G. Rivolta, G. Chini Zittelli, N. Bassi, L. Rodolfi, D. Casini, M. Prussi, D. Chiaramonti, M.R. Tredici, Oil production by the marine microalgae *Nannochloropsis* sp. F & M-M24 and *Tetraselmis suecica* F & M-M33, Bioresour. Technol. 114 (2012) 567–572, http://dx.doi.org/10.1016/j.biortech.2012.02.123.

[9] G. Breuer, P.P. Lamers, D.E. Martens, R.B. Draaisma, R.H. Wijffels, Effect of light intensity, pH, and temperature on triacylglycerol (TAG) accumulation induced by nitrogen starvation in Scenedesmus obliquus, Bioresour. Technol. 143 (2013) 1–9, http://dx.doi.org/10.1016/j.biortech.2013.05.105.

[10] G. Breuer, L. de Jaeger, V.P.G. Artus, D.E. Martens, J. Springer, R.B. Draaisma, G. Eggink, R.H. Wijffels, P.P. Lamers, Superior triacylglycerol (TAG) accumulation in starchless mutants of Scenedesmus obliquus: (II) evaluation of TAG yield and productivity in controlled photobioreactors, Biotechnol. Biofuels 7 (2014) 70, http://dx.doi.org/10.1186/1754-6834-7-70.

[11] G. Breuer, P.P. Lamers, M. Janssen, R.H. Wijffels, D.E. Martens, Opportunities to improve the areal oil productivity of microalgae, Bioresour. Technol. 186 (2015) 294–302, http://dx.doi.org/10.1016/j.biortech.2015.03.085.

[12] I.T.D. Cabanelas, M.V.D. Zwart, D.M. Kleinegris, R.H. Wijffels, M.J. Barbosa, Sorting cells of the microalga *Chlorococcum littorale* with increased triacylglycerol productivity, Biotechnol. Biofuels. (2016), http://dx.doi.org/10.1186/s13068-016-0595-x.

[13] M. Chihara, T. Nakayama, I. Inouye, M. Kodama, *Chlorococcum littorale*, a new marine green coccoid alga (Chlorococcales, Chlorophyceae), Arch. Protistenkd. 144 (1994) 227–235, http://dx.doi.org/10.1016/S0003-9365(11)80133-8.

[14] Y. Chisti, Biodiesel from microalgae beats bioethanol, Trends Biotechnol. 26 (2008) 126–131, http://dx.doi.org/10.1016/j.tibtech.2007.12.002.

[15] R. Davis, A. Aden, P.T. Pienkos, Techno-economic analysis of autotrophic microalgae for fuel production, Appl. Energy 88 (2011) 3524–3531, http://dx.doi.org/10.1016/j.apenergy.2011.04.018.

[16] J.H. de Vree, R. Bosma, M. Janssen, M.J. Barbosa, R.H. Wijffels, Comparison of four outdoor pilot-scale photobioreactors, Biotechnol. Biofuels 8 (2015) 215, http://dx.doi.org/10.1186/s13068-015-0400-2.

[17] M. Dubois, K.A. Gilles, J.K. Hamilton, P.A. Rebers, F. Smith, Colorimetric method for determination of sugars and related substances, Anal. Chem. 28 (1956) 350–356.

[18] J. Fábregas, A. Maseda, A. Domínguez, M. Ferreira, A. Otero, Changes in the cell composition of the marine microalga, Nannochloropsis gaditana, during a light:-dark cycle, Biotechnol. Lett. 24 (2002) 1699–1703, http://dx.doi.org/10.1023/A:1020661719272.

[19] A.K. Gombert, J. Nielsen, Mathematical modelling of metabolism, Curr. Opin. Biotechnol. 11 (2000) 180–186, http://dx.doi.org/10.1016/S0958-1669(00)00079-3.

[20] M.J. Griffiths, R.P. Hille, S.T.L. Harrison, Lipid productivity, settling potential and fatty acid profile of 11 microalgal species grown under nitrogen replete and limited conditions, J. Appl. Phycol. 24 (2012) 989–1001, http://dx.doi.org/10.1007/s10811-011-9723-y.

[21] J.U. Grobbelaar, L. Nedbal, V. Tichý, Influence of high frequency light/dark fluctuations on photosynthetic characteristics of microalgae photoacclimated to different light intensities and implications for mass algal cultivation, J. Appl. Phycol. 8 (1996) 335–343, http://dx.doi.org/10.1007/BF02178576.

[22] Q. Hu, M. Kawachi, I. Iwasaki, S. Miyachi, N.K., Ultrahigh-cell-density culture of a marine green alga *Chlorococcum littorale* in a flat-plate photobioreactor, Appl. Microbiol. Biotechnol. 49 (1998) 655–662.

[23] X. Johnson, J. Alric, Central carbon metabolism and electron transport in *Chlamydomonas reinhardtii*: metabolic constraints for carbon partitioning between oil and starch, Eukaryot. Cell 12 (2013) 776–793, http://dx.doi.org/10.1128/EC.00318-12.

[24] A.J. Klok, D.E. Martens, R.H. Wijffels, P.P. Lamers, Simultaneous growth and neutral lipid accumulation in microalgae, Bioresour. Technol. 134 (2013) 233–243, http://dx.doi.org/10.1016/j.biortech.2013.02.006.

[25] A.J. Klok, P.P. Lamers, D.E. Martens, R.B. Draaisma, R.H. Wijffels, Edible oils from microalgae: insights in TAG accumulation, Trends Biotechnol. 32 (2014) 521–528, http://dx.doi.org/10.1016/j.tibtech.2014.07.004.

[26] Norihide Kurano, S.M., Selection of microalgal growth model for describing specific growth rate-light response using extended information criterion, J. Biosci. Bioeng. 100 (2005) 403–408.

[27] K.J. McCree, Photosynthetically active radiation, Physiological Plant Ecology, Springer, Berlin, Heidelberg, 1981, pp. 41–55, , http://dx.doi.org/10.1007/978-3-642-68090-8_3.

[28] I.A. Nascimento, S.S.I. Marques, I.T.D. Cabanelas, S.A. Pereira, J.I. Druzian, C.O. de Souza, D.V. Vich, G.C. de Carvalho, M.A. Nascimento, Screening microalgae strains for biodiesel production: lipid productivity and estimation of fuel quality based on fatty acids profiles as selective criteria, Bioenergy Res. 6 (2013) 1–13.

[29] N.H. Norsker, M.J. Barbosa, M.H. Vermue, R.H. Wijffels, Microalgal production—a close look at the economics, Biotechnol. Adv. 29 (2011) 24–27, http://dx.doi.org/10.1016/j.biotechadv.2010.08.005.

[30] J. Pruvost, G. Van Vooren, G. Cogne, J. Legrand, Investigation of biomass and lipids production with Neochloris oleoabundans in photobioreactor, Bioresour. Technol. 100 (2009) 5988–5995, http://dx.doi.org/10.1016/j.biortech.2009.06.004.

[31] C. Rigollier, M. Lefèvre, L. Wald, The method Heliosat-2 for deriving shortwave solar radiation from satellite images, Sol. Energy 77 (2004) 159–169, http://dx.doi.org/10.1016/j.solener.2004.04.017.

[32] L. Rodolfi, G.C. Zittelli, N. Bassi, G. Padovani, N. Biondi, G. Bonini, M.R. Tredici, Microalgae for oil: strain selection, induction of lipid synthesis and outdoor mass cultivation in a low-cost photobioreactor, Biotechnol. Bioeng. 102 (2009) 100–112, http://dx.doi.org/10.1002/bit.22033.

[33] A. San Pedro, C.V. González-López, F.G. Acién, E. Molina-Grima, Marine microalgae selection and culture conditions optimization for biodiesel production, Bioresour. Technol. 134 (2013) 353–361, http://dx.doi.org/10.1016/j.biortech.2013.02.032.

[35] P.M. Slegers, M.B. Lösing, R.H. Wijffels, G. van Straten, A.J.B. van Boxtel, Scenario evaluation of open pond microalgae production, Algal Res. 2 (2013) 358–368, http://dx.doi.org/10.1016/j.algal.2013.05.001.

[36] P.M. Slegers, P.J.M. van Beveren, R.H. Wijffels, G. van Straten, A.J.B. van Boxtel, Scenario analysis of large scale algae production in tubular photobioreactors, Appl. Energy 105 (2013) 395–406, http://dx.doi.org/10.1016/j.apenergy.2012.12.068.

[37] G. Torzillo, A. Sacchi, R. Materassi, A. Richmond, Effect of temperature on yield and night biomass loss in spirulina platensis grown outdoors in tubular photobioreactors, J. Appl. Phycol. 3 (1991) 103–109, http://dx.doi.org/10.1007/BF00003691.

[38] M.R. Tredici, Photobiology of microalgae mass cultures: understanding the tools for the next green revolution, Biofuels 1 (2010) 143–162, http://dx.doi.org/10.4155/bfs.09.10.

[39] M.R. Tredici, G.C. Zlttelli, Efficiency of sunlight utilization: tubular versus flat photobioreactors, Biotechnol. Bioeng. 57 (1998) 187–197, http://dx.doi.org/10.1002/(SICI)1097-0290(19980120)57:2<187::AID-BIT7>3.0.CO;2-J.

[40] G. Van Vooren, F. Le Grand, J. Legrand, S. Cuiné, G. Peltier, J. Pruvost, Investigation of fatty acids accumulation in Nannochloropsis oculata for biodiesel application, Bioresour. Technol. 124 (2012) 421–432, http://dx.doi.org/10.1016/j.biortech.2012.08.009.

[41] R.H. Wijffels, M.J. Barbosa, An outlook on microalgal biofuels, Science 329 (2010) 796–799, http://dx.doi.org/10.1126/science.1189003 (80-.).